Supplementary Information for

$Fe_{1-x}S$/C nanocomposites from sugarcane waste-derived microporous carbon for high-performance lithium ion batteries

Chundong Wang,[abc] Minhuan Lan,[c] Yi Zhang,[d] Haidong Bian,[c] Muk-Fung Yuen,[c] Kostya (Ken) Ostrikov,[ef] Jianjun Jiang,[a] Wenjun Zhang,[c] Yang Yang Li[c*] and Jian Lu[b*]

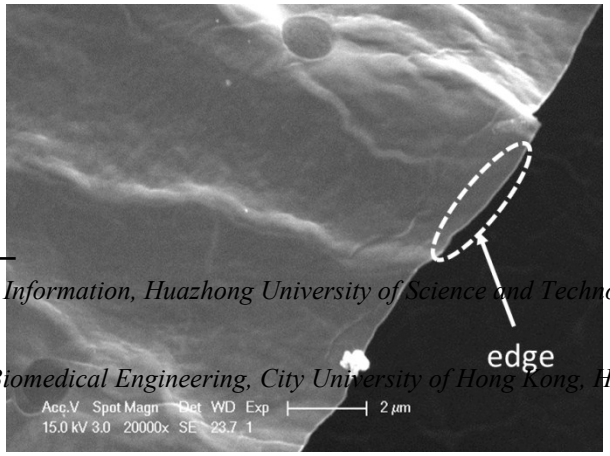

Fig. S1 SEM image of carbon sheets in microporous carbon (MC) with the thin and flexible edge indicated.

[a] *School of Optical and Electronic Information, Huazhong University of Science and Technology, Wuhan 430074, P.R. China*

[b] *Department of Mechanical and Biomedical Engineering, City University of Hong Kong, Hong Kong SAR, P.R. China*

[c] *Center of Super-Diamond and Advanced Films (COSDAF), Department of Physics and Materials Science, City University of Hong Kong, Hong Kong SAR, P.R. China*

[d] *School of Chemical Engineering and Pharmacy, Wuhan Institute of Technology, Wuhan, 430073, P.R. China*

[e] *School of Chemistry, Physics and Mechanical Engineering, Queensland University of Technology, Brisbane, Queensland 4000, Australia*

[f] *Plasma Nanoscience, Industrial Innovation Program, CSIRO Manufacturing Flagship, Lindfield, New South Wales 2070, Australia*

Author to whom correspondence should be addressed. E-mail: yangli@cityu.edu.hk (Y.Y. Li), jianlu@cityu.edu.hk (J. Lu)

† Electronic supplementary information (ESI) available. See DOI: XXX

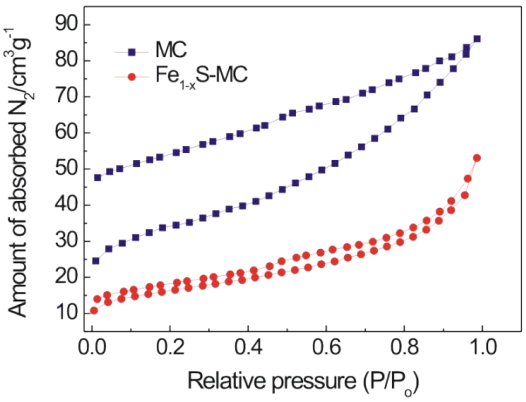

Fig. S2 Nitrogen adsorption–desorption isotherms of microporous carbon and $Fe_{1-x}S$-MC at 77 K.

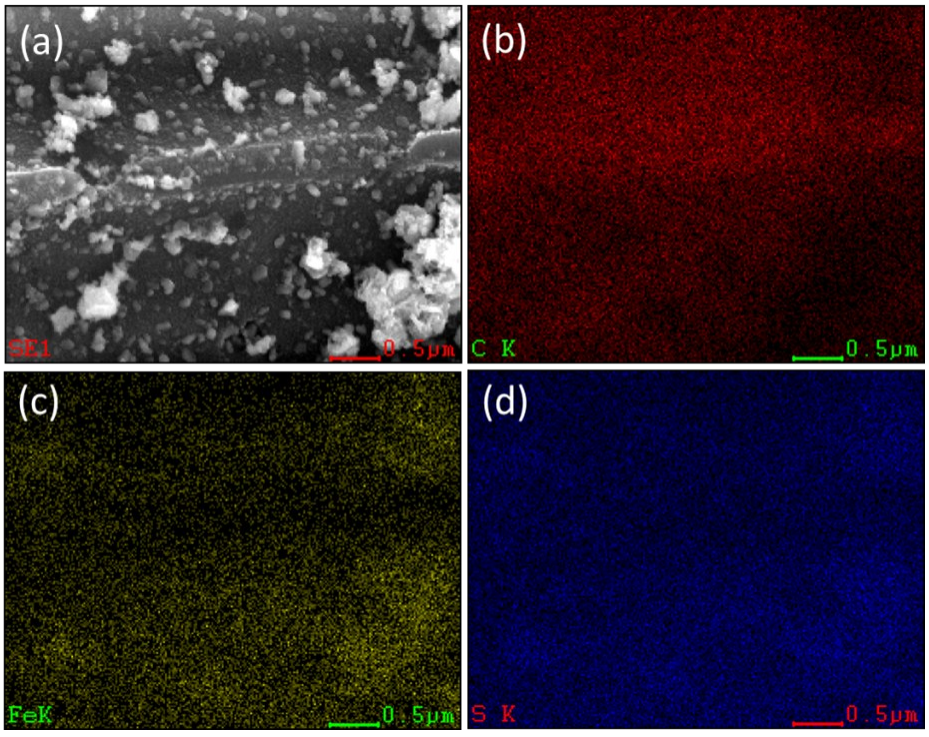

Fig. S3 EDX mapping of Fe_{1-x} S-MC, suggesting the uniform distribution of the $Fe_{1-x}S$ nanoparticles on MC.

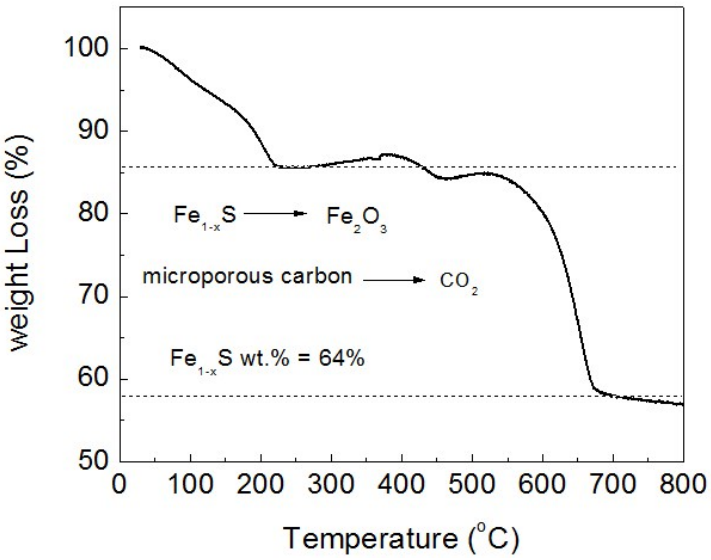

Fig. S4 The TGA curve of the FeS_{1-x}-MC nanocomposites.

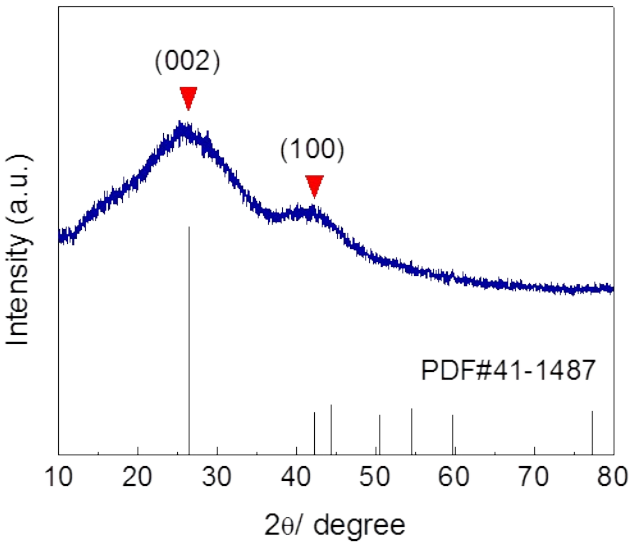

Fig. S5 XRD pattern of microporous carbon.

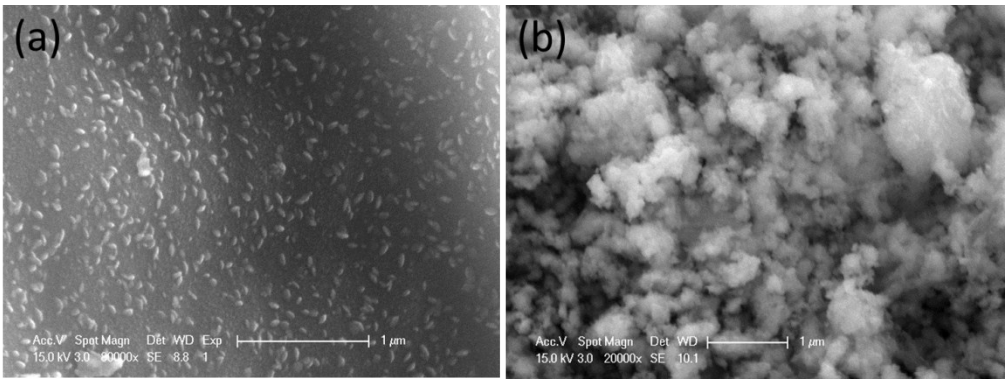

Fig. S6 SEM images of the as-synthesized HT product (a) and $Fe_{1-x}S$ particles (b).

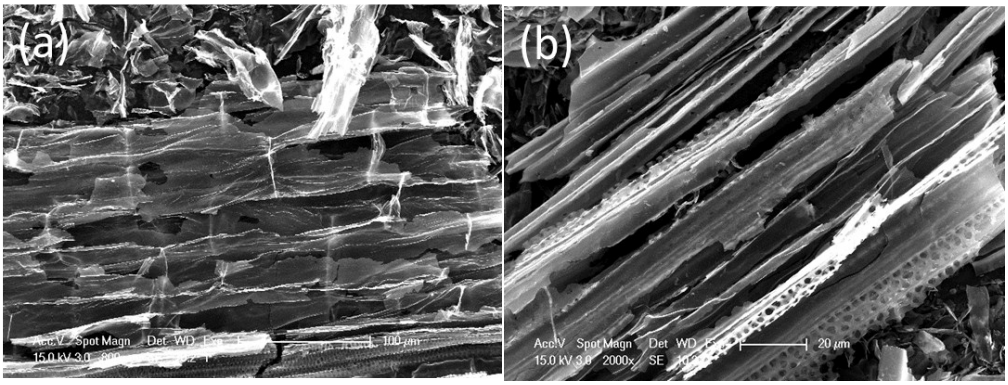

Fig. S7 SEM images of microporous carbon after surface functionalization through acid treatment.

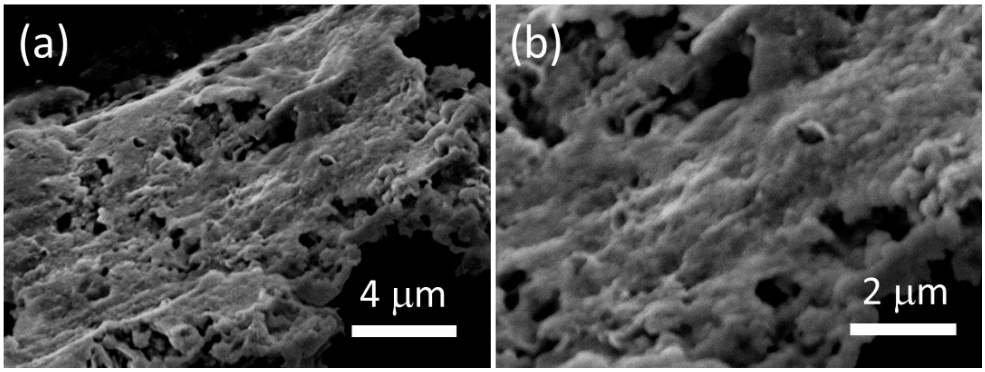

Fig. S8 SEM images of the $Fe_{1-x}S$-MC nanocomposite after 200 LIB charging/discharging cycles at 100 mA g^{-1}.

Table S1 Cycling performance comparison of the iron sulfide-based LIB anodes tested at constant current densities.

Anode structure	Current density (mAg^{-1})	Specific capacity ($mAhg^{-1}$)	Cycle #	Capacity retention (%)	Year Published	Reference
Ultrathin C@FeS nanosheets	100	615	100	99	2012	[48]
FeS-embedded carbon microsphere	50	736	50	77	2011	[49]
TiO_2 modified FeS	100	635	100	>100	2013	[59]
High energy milled FeS	(0.05 mA/ cm^2)	522	15	95	2005	[60]

RGO wrapped FeS nanocomposites	100	978	40	90	2013	[55]
FeS microsheet networks	100	677	20	97	2015	[61]
FeS/C-3wt%Bi_2O_3	300	325	200	99.2	2015	[62]
core–shell Fe_7S_8@C	100	695	50	–	2015	[63]
$Fe_{1-x}S$ -MC	**100**	**1185**	**200**	**142**	**--**	**This work**
	300	**630**	**40**	**97**		